Heterogeneous Connectivity Patterns Alter the Timing Variability in Spatially Distributed Dynamic Systems

Viktor K. Jirsa

Center for Complex Systems & Brain Sciences, Florida Atlantic University, 777 Glades Road, Boca Raton FL 33444 USA

E-mail: jirsa@walt.ccs.fau.edu

(Received 21 October 2002)

Heterogeneous connectivity is omnipresent in spatially distributed biological systems. This property allows to introduce an information processing hierarchy in a spatially continuous system by means of organizing its spatiotemporal dynamics. The brain with its intricate and detailed connectivity is a beautiful example. In particular, it is understood that neuronal spike firings of action potentials contribute to the information processing in the brain. Here we ask the question, how the variability of these firing patterns is altered by the introduction of a heterogeneous fiber system. We study the special case of a two-point connection.

Key words: spatiotemporal dynamics, neural fields, heterogeneous connectivity, variability

PACS numbers: 87.18.Sn, 47.54.+r, 82.40.k, 84.35.+i

1 Introduction

Historically, macroscopic pattern formation and self-organization phenomena have been studied systematically in physical and chemical systems (see Ref. [1, 4] for reviews). One of the pioneers in the field, Hermann Haken, has not only developed methodological aspects of self-organization phenomena, but also, most importantly, conceptual and philosophical entry points captured under the collective expression Synergetics. Many examples can be found in physics, e.g. hydrodynamics, laser, and chemistry, e.g. Belousov Zhabotinsky reaction. One of the strengths of Synergetics is the dual approach though, that is the complementary bottom-up and the top-down approaches. The bottom-up approach starts with a discussion of the microscopic dynamics of a complex system and leads to the derivation of the macroscopic order parameters. The top-down approach assumes the existence of an order parameter dynamics and provides an entry point to phenomenological modelling using a rich inventory of mathematical tools. Especially the latter approach has proved to be powerful in understanding collective phenomena in disciplines, in which the microscopic dynamics is typically not known. By doing so, Hermann Haken has entered, or shall I say "created", the field of rigorous mathematical modelling in the Life sciences, such as human movement sciences [2] and brain sciences [3, 11]. Of course, there have been many other phenomenological modelling approaches throughout the literature, but none of them has been supported by such a systematic formalism as the one provided by Synergetics.

In the following I wish to pick up the following line of thinking: Biological systems such as brain tissue consisting of billions of neural cells display phenomena of pattern formation and self-organization. These cells communicate with each other and process information over time. The timing of these processes at different sites will certainly influence the overall pattern, which emerges, and hence the entire information processing. How do these different sites communicate and how is their timing affected by this communication? Brain tissue has the property, that areas are not only locally connected, but also globally. Such long-range interactions may also be found in physical systems, but the interaction patterns of the latter show always

translational invariance in space. This is different for brain tissue. If area A is connected to area B over a distance d, then area C, which has also a distance d to area B, does not necessarily connect (directly) to B. This property of a mutual presence of spatially invariant local connections and spatially variant long-range connections is omnipresent in the brain. In physical systems, to the extent that inhomogeneous properties are considered, they are typically introduced as spatially varying parameters or inputs to the homogeneous system (see e.g. Ref. [5] for a recent example). Systems with a spatially invariant connection topology allow for a differential partial differential description of their dynamics. This is not the case for systems, which we encounter in general life sciences. Neuronal networks, biological tissue and geographic spread of epidemics (see [16] for an introduction) are just a few other examples. In such cases, a description of the dynamics as a partial differential equation results in high order differentials and a multitude of delays raising the complexity enormously. An integral description, however, allows for spatiotemporal pattern formation and provides a simpler representation and control of the inhomogeneous connection topology by its integral kernel. An initial treatment of an inhomogeneous connection topology in a dynamic system has been made by the introduction of instantaneous long-range connections between areas in a discretely coupled chain of oscillators [6]. In previous work [7, 8] we have reported an integral formulation of a spatially continuous dynamic system with a heterogeneous connection topology and propagation delays along its connections. Experimentally, these systems are probed by detectors at specific locations. These detectors register the on-going activity simultaneously at each site. After data collection, the analysis of the timing and its variability between individual sites provides information on how sites communicate with each other and how they are connected. A reduced variability in the timing of events between different locations is typically understood to be a consequence of the presence of a coupling and thus enhanced information exchange. However, the question remains open how different couplings or pathways influence the timing variability. The emergence of a spatiotemporal pattern will naturally reduce the timing variability. In previous work [7, 8], we showed that the introduction of additional pathways may induce macroscopic pattern formation implying a reduced timing variability. In the present study, we investigate the contributions of homogeneous and heterogeneous couplings below, but close to the threshold of macroscopic pattern formation, however in the presence of noise. In particular we study the communication between individual sites from the modelling perspective, that is we define a spatiotemporal system with a homogeneous connectivity and embed an additional pathway connecting two sites A and B. Then we study the timing of activation and its variability at the individual sites in dependence of the presence or non-presence of a direct pathway between A and B. In paragraph 2 we briefly review the formalism [7] which allows such a system's analytic treatment of pattern formation by means of a mode decomposition. In paragraph 3 the paradigmatic example of a two-point connection embedded in a continuous homogeneously connected medium illustrates the destabilization mechanism of a heterogeneous connection. The destabilization leads to a non-equilibrium phase transition and causes macroscopic pattern formation. In paragraph 4 we show how the variability of the timing between individual areas is affected by different types of connectivity.

2 Dynamics of integral equations

We define the spatiotemporal dynamics of a scalar field $\psi(x,t)$ with space $x \in \mathcal{R}^n$ and time $t \in \mathcal{R}$ as a nonlinear retarded integral equation of the form

$$\psi(x,t) = \int_A dX f(x,X) S(\psi(X,T) + I(X,T)) \quad (1)$$

where $f(x,X)$ describes a general connectivity function and S a nonlinear function of ψ at space-point X and a time-point $T = t - |x-X|/v$ delayed by the propagation time over the distance $|x-X|$. A denotes the surface area of the medium and v the constant signal velocity. $I(t)$ is the input to the field $\psi(x,t)$. Variations of this type of integral equation have been widely used in theoretical neuroscience [9, 10, 11, 12, 13] to describe the dynamics of neural activity. But in all these cases, as well as generally in physical systems, translational variance $f(x,X) = f(|x-X|)$ has been employed.

Here we assume $f(x,X)$ to be a general function of x and X. We decompose the field $\psi(x,t)$ into spatial modes $g_n(x)$ and complex time dependent amplitudes $\psi_n(t)$ such as

$$\psi(x,t) = \sum_{n=-\infty}^{\infty} g_n(x)\psi_n(t) \tag{2}$$

The choice of the spatial basis functions will depend on the surface A and its boundary conditions, but also on practical considerations about the type of connectivity $f(x,X)$ and inputs I to the system. An adjoint basis is given by

$$\int_A dx\ \bar{g}_m(x)g_n(x) = \delta_{mn} \tag{3}$$

where δ_{mn} is the Kronecker symbol. We choose a polynomial representation of the nonlinear function S in (1) such as

$$\begin{aligned} S(X,T) &= a_0 + a_1\psi(X,T) + a_2\psi^2(X,T) \\ &\quad +... = \sum_{m=0}^{\infty} a_m\psi^m(X,T) \end{aligned} \tag{4}$$

where $a_m \in \mathcal{R}$ and $I(X,T)$ is not considered (no restriction of generality). By projection of (1) on a spatial basis function $\bar{g}_q(x)$ and restricting its dimension N to be finite, we obtain a set of N coupled integral equations

$$\begin{aligned} \psi_q(t) &= \int_A dx\ \bar{g}_q(x) \int_A dX\ f(x,X) \sum_{m=0}^{\infty} a_m \\ &\quad \times (\sum_{n=-N}^{N} g_n(X)\psi_n(T))^m \end{aligned} \tag{5}$$

Note that T still depends on the distance $|x-X|$. We perform the following trick: exchange space and time integration by introducing a time integral and a δ-function $\delta(t-\tau-v^{-1}|x-X|)$ in (5); then perform the integration over dX preserving $t-\tau \geq 0$ for causality. The resulting equations are

$$\begin{aligned} \Psi(t) &= v\int_{-\infty}^{t} d\tau\ (\Gamma_0(t-\tau) + \Gamma_1(t-\tau)\Psi(\tau) \\ &\quad +\Gamma_2(t-\tau)\Psi(\tau)\Psi(\tau) + ...) \\ &= v\int_{-\infty}^{t} d\tau\ \Gamma_0(t-\tau) + L^t\Psi(t) + N^t(\Psi(t)) \end{aligned} \tag{6}$$

where vector notation has been used:

$$\Psi(t) = (\cdots\psi_q(t)\cdots)^T \tag{7}$$

and

$$\begin{aligned} \Gamma_0(t-\tau) &= (\cdots\Gamma_q(t-\tau)\cdots)^T \\ \Gamma_1(t-\tau) &= (\cdots\Gamma_{qn}(t-\tau)\cdots) \\ &\vdots \end{aligned} \tag{8}$$

Formally L^t and N^t represent the linear and nonlinear temporal evolution operators. The tensor matrix elements are

$$\begin{aligned} \Gamma_q(t-\tau) &= a_0(\gamma_q^-(t-\tau) + \gamma_q^+(t-\tau)) \\ \Gamma_{qn}(t-\tau) &= a_1(\gamma_{qn}^-(t-\tau) + \gamma_{qn}^+(t-\tau)) \\ &\vdots \end{aligned} \tag{9}$$

where

$$\begin{aligned} \gamma_q^{\pm}(t-\tau) &= \int_A dx\ \bar{g}_q(x)f(x,x\pm v(t-\tau)) \\ \gamma_{qn}^{\pm}(t-\tau) &= \int_A dx\ \bar{g}_q(x)f(x,x\pm v(t-\tau)) \\ &\quad \times g_n(x\pm v(t-\tau)) \\ &\vdots \end{aligned} \tag{10}$$

Our particular interest is in macroscopic phase transitions from one mode to another, i.e. the destabilization of a stationary spatiotemporal state. We consider a stationary solution Ψ_0 of (6) and its small deviations $\epsilon(t)$ resulting in $\Psi(t) = \Psi_0 + \epsilon(t)$. Then (6) may be written as

$$\begin{aligned} \epsilon(t) &= L^t\Psi(t) + N^t(\Psi(t)) - L^t\Psi_0 + N^t(\Psi_0) \\ &= \tilde{L}^t\epsilon(t) + \tilde{N}^t(\epsilon(t)) \end{aligned} \tag{11}$$

where $\tilde{N}^t(\epsilon(t))$ is of the order $|\epsilon|^2$. The general solution of the linear parts of (11) is

$$\epsilon(t) = \sum_{n=1}^{N}(\sum_{m=0}^{M-1} c_{mn}t^m)e^{\lambda_n t}O_n \tag{12}$$

where c_{mn} is a constant, λ_n the eigenvalue, M its multiplicity and O_n the right-hand eigenvector. The eigenvalue problem of (11) is defined as

$$\det(e^{-\lambda t}L^t(e^{-\lambda\tau}) - I) = 0 \tag{13}$$

and provides λ_n. The identity matrix is I. Decomposing $\epsilon(t) = \sum_{i=1}^{N} \xi_i(t) O_i$ and defining the left-hand eigenvectors $\bar{O}_k$ of the linear problem in (11) we obtain by projecting (11) on $\bar{O}_k$

$$\xi_k(t) = \int_{-\infty}^{t} \lambda_k \xi_k(\tau) d\tau + \bar{O}_k \tilde{N}^t (\sum_{i=1}^{N} \xi_i(\tau) O_i) \quad (14)$$

The nonlinear contributions can be rewritten such that

$$\xi_k(t) = \int_{-\infty}^{t} d\tau \; (\lambda_k \xi_k(\tau) + \sum_{rs=1}^{N} \bar{\Gamma}_{2krs}(t-\tau) \xi_r(\tau) \xi_s(\tau) + \text{higher orders}) \quad (15)$$

with

$$\bar{\Gamma}_{2krs}(t-\tau) = \sum_{jmn=1}^{N} \bar{O}_k^j \Gamma_{2jmn}(t-\tau) O_r^m O_s^n \quad (16)$$

where the superscript of the eigenvectors denotes their elements. Here the entire complexity of the connection topology is contained in the tensor matrices $\bar{\Gamma}$ which can be explicitly expressed as integrals of the connectivity $f(x, X)$ and the spatial basis functions $\bar{g}_n(x), g_m(x)$. The linear stability of an eigen mode $\xi_k(t)$ is determined by its eigenvalue λ_k. Thus we are able to express the entire dynamics of (1) in terms of its eigen modes under appropriate choice of $\bar{g}_n(x), g_m(x)$ in the vicinity of a phase transition.

3 Influence of a two-point connection

Let us now consider the example of a one-dimensional homogeneous medium with a heterogeneous two-point connection between locations x_1 and x_2. The connectivity function $f(x, X)$ shall be given by

$$f(x, X) = f(|x - X|) + f_{12}(x, X) + f_{21}(x, X) \quad (17)$$

where f_{12} is the link from x_2 to x_1 and f_{21} the link in the opposite direction as illustrated in figure 1. The distance between the inhomogeneous contributions of connectivity is $d = |x - X|$ which serves as our control parameter.

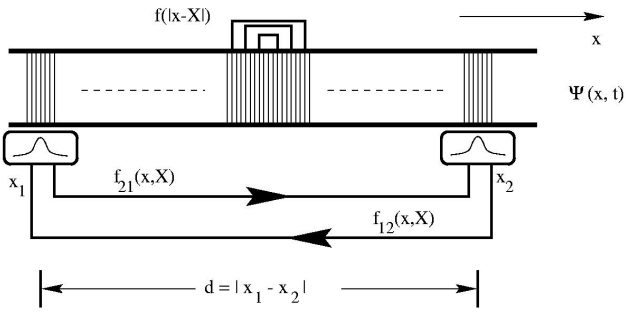

FIG. 1. Two-point connection. The homogeneous connection topology is illustrated within a one-dimensional continuous medium whose activity is described by $\psi(x, t)$. A projection from x_1 to x_2 introduces a heterogeneity into the connectivity.

The dynamics of our example is given by

$$\psi(x, t) = a \int_A dX f(x, X) S(\psi(X, T) - \bar{\psi}(X, T)) \quad (18)$$

with $T = t - |x - X|/v$ and $x, X \in \mathcal{R}$. $\bar{\psi}(x, t) = \int_A dX \; \psi(X, t)$ is subtracted to reduce spatially uniform saturation effects [11]. Periodic boundaries are imposed. The connectivities are specified as

$$\begin{aligned} f(|x - X|) &= f_0 e^{-|x-X|/\sigma} \\ f_{ij}(x, X) &= f_{ij} \delta(x - x_i) \delta(X - x_j) \; i \neq j \end{aligned} \quad (19)$$

where $a, \sigma, f_{12}, f_{21}$ are constant parameters. We choose the spatial basis system to be spanned by the trigonometric functions $\sin nkx, \cos mkx$ with $n, m \in \mathcal{Z}$ and $k = 2\pi/L$ where L is the length of the one-dimensional closed loop. $x_1 = 0$ is not varied thereby resulting in pinning of the spatial modes around $x = 0$. The nonlinear function S in (18) is assumed to be sigmoidal [11]. We study the stability of the origin $\Psi_0 = 0$ and expand S around its deflection point, $S[n] \approx \alpha n - 4/3\alpha^3 n^3 \pm \cdots$. We consider spatial basis function $g_m(x) = \cos mkx$ to 2nd order in m and truncate the expansion of the sigmoid after the 3rd order studying small amplitude dynamics. Application of (6) - (16) provides the following eigenvalue problem

$$v \int_{-\infty}^{t} d\tau \; e^{-im\omega(t-\tau)} \Gamma_{mm}(t-\tau) e^{-\lambda_m(t-\tau)} = 1 \quad (20)$$

where ω is a constant, m refers to the spatial mode number and

$$\Gamma_{mm}(t-\tau) = \frac{a\alpha}{\sigma} e^{-\omega_0(t-\tau)} \cos mkv(t-\tau) + d_1\delta(|x_1 - x_2| - v(t-\tau)) \quad (21)$$

where

$$d_1 = a\alpha/L(\frac{f_{12}f_{21}}{f_{12}+f_{21}}) \cos mkx_1 \cos mkx_2 \quad (22)$$

Inserting (21) in (20) provides us with a transcendental equation for $z = \lambda_m + im\omega$

$$\left(z^2 + 2\omega_0 z + \omega_0^2 + m^2k^2v^2\right)\left(1 - d_1 e^{zd/v}\right) - (z+\omega_0)\omega_0 a\alpha = 0 \quad (23)$$

The real part λ_m of the eigenvalue z of the m-th mode and its frequency ω can be determined graphically from (23) as a function of the control parameter d. The destabilization of a particular state m depends on d_1 and d. For $d_1, d = 0$ the purely homogeneous system is obtained in which the origin is the only stable state for sufficiently small α. The introduction of a heterogeneous projection $f_{ij}(x, X)$ may cause a desynchronization of the connected areas and thus a destabilization of the respective spatial mode resulting in a phase transition. The desynchronization properties are determined by the tensor matrices in (10) which describe the interplay of the connectivity and distribution of areas represented as spatial modes. This interplay prescribes the timing relationship of activity between areas via the time delay and thus determines its desynchronizing properties.

4 Variability of timing patterns

We study the the timing and its variability in dependence of the presence of a two-point connection. The connectivity matrix is defined by (17),(19) and illustrated in figure 2. In addition to the influence of the connectivity, given in (1), we allow for an intrinsic dynamics at each site, that is independent of the neighboring active elements. Here we choose the intrinsic dynamics to be an excitable medium, for instance of Fitz-Hugh Nagumo (FHN) type [14, 15]. Then the activation $\psi(x,t)$ is described by two variables $\psi(x,t) = (u(x,t), v(x,t))$

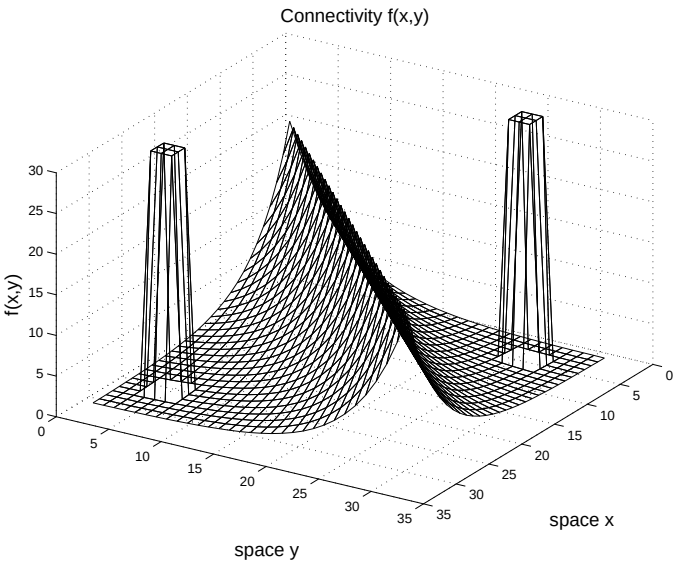

FIG. 2. Connectivity matrix $f(x,y)$ with homogeneous contributions and the bilateral two-point connection. The latter appears as the two singularities f_{12} and f_{21} in the connectivity matrix.

for which only the first component, the excitatory u, has connections, the other component, the inhibitory v, is local. Then the system after expansion of $\psi(x, t+\Delta t)$ into a Taylor series assuming $\Delta t \ll 1$ reads

$$\dot{\psi}(x,t) \approx F(\psi(x,t)) + \int_A dX f(x,X) S(\psi(X,T)) \quad (24)$$

with $F(\psi(x,t))$ as the intrinsic FHN dynamics. The explicit equations are

$$\dot{u} = c_1(u - u^3/3 - v + I_1) + \int_A dX f(x,X) S(u-\bar{u})(X,T) \quad (25)$$

$$\dot{v} = c_2(-v + \frac{5}{4}u + I_2) \quad (26)$$

The parameters are $c_1 = 10, c_2 = 0.8, I_2 = 1.5$. I_1 may vary in space and time, but will chosen here to excite one particular site in the medium constantly, $I_2 = 0.2$, and being zero otherwise. The connectivity parameters are $f_0 = 20, f_{12} = f_{21} = 30, \sigma = 0.5$. The time T in the connectivity integral is $T = t - |x - X|/v$. For a formal analysis of the intrinsic FHN dynamics we refer, for instance, to [17].

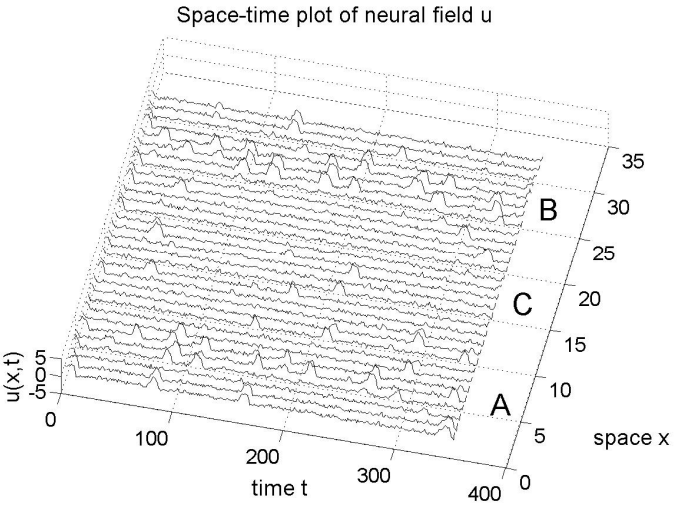

FIG. 3. Dynamics of the activity of $u(x,t)$ over space and time. The connectivity has a homogeneous component and a bilateral pathway between sites A and B. Note the enhanced clustering of spike occurences at these sites in comparison to site C.

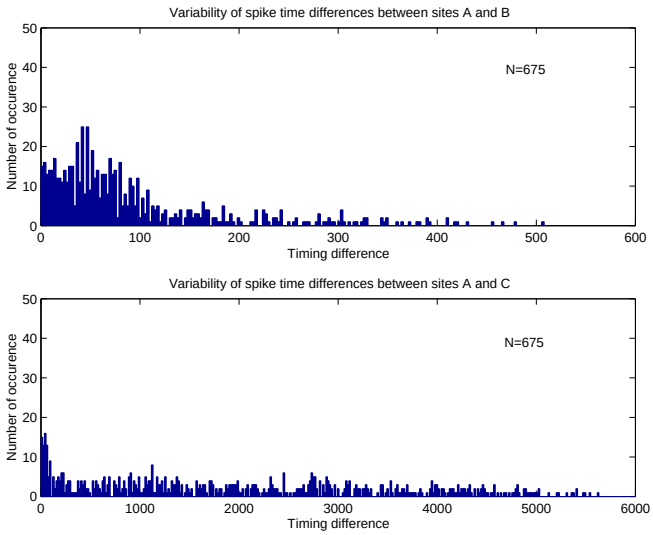

FIG. 4. Homogeneous projections are present only ($f_0 = 20, f_{12} = f_{21} = 0$). The distributions show a modest clustering of timing differences around its intrinsic firing rates.

In principle, there is a separatrix in phase space for which the FHN system shows properties of an excitable medium: Below a threshold value of u the system relaxes to a fixed point, but above this value the system gets excited, emits a large amplitude spike and returns eventually to the fixed point. The inclusion of additive noise in space and time turns equations (25, 26) into a stochastic system and allows for a random emission of spikes. The present parameter space is chosen such that the origin, that is $u(x,t) = 0\ \forall x$, is stable. However, the proximity to the threshold, when the origin gets destabilized, is expected to cause a spatially non-uniform distribution of events in the stochastic system.

We focus on the following question: Given three sites A, B and C in the active medium (see figure 3), how does the inclusion of an additional two-point connection from A to B render the variability of the occurrence of spike timings for a given noise level? The site C shall be located somewhere far from A, B and we will study the variability of the time difference of spikes between A and B, as well as between A and C. In figure 3 we illustrate the spatiotemporal dynamics of the activity $u(x,t)$ while a bilateral pathway connects sites A and B. Just from visual inspection, it is evident that a clustering of spikes occurs at these sites over time. Spikes occur more frequently with a fixed time lag between A and B, rather than between A and C. Our aim is to quantify this observation. We will compare four situations: 1) homogeneous connectivity only; 2) homogeneous connectivity and a one-way projection from A to B; 3) homogeneous connectivity and a bilateral pathway between A and B, that is feed forward and feed backward; 4) bilateral pathway between A and B only, that is all the active units in between are disconnected. For each of these four scenarios we study the difference $\Delta t = \min(|t_A - t_{B,C}|)$ between the time of occurrence of a spike at sites A and B or C, respectively. The distribution of the timing difference Δt between sites provides information on the amount of communication exchanged between areas in the noisy environment. Our interest is to identify which mechanism may be used to obtain an increased degree of synchronization, that is a reduced variability in the timing difference.

4.1 Homogeneous connectivity only

If no heterogeneous pathways are present, then the connectivity is translationally invariant. The connectivity still has a spatial structure, in this case excitatory connections decaying with increasing dis-

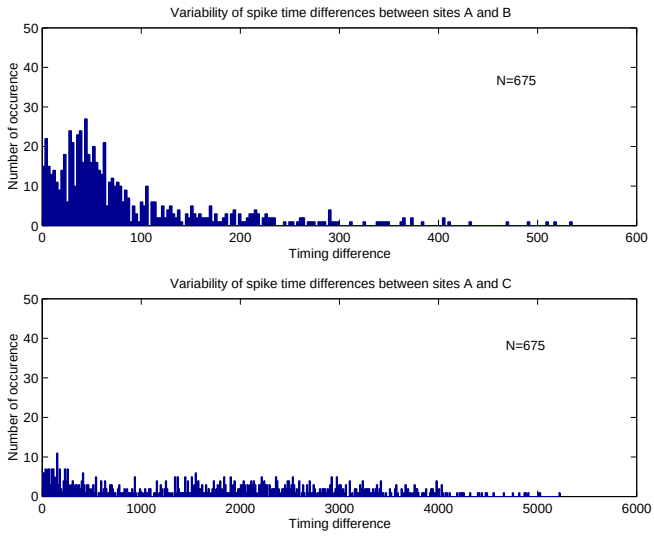

FIG. 5. Homogeneous connectivity and a uni-directional projection from A to B ($f_0 = 20, f_{12} = 30, f_{21} = 0$).

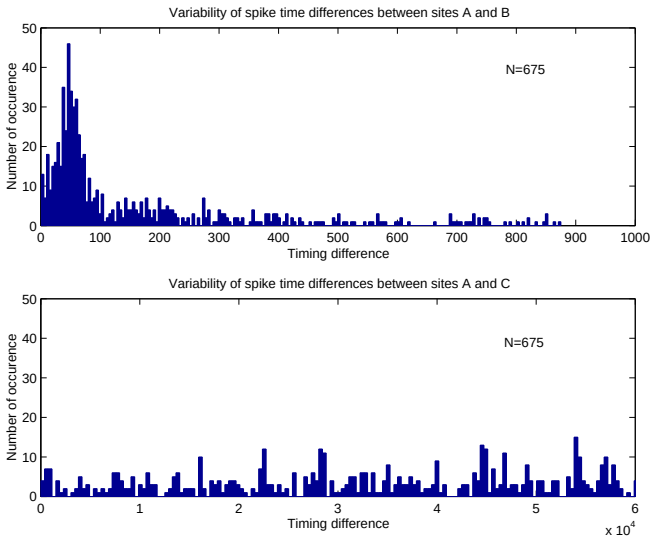

FIG. 6. Homogeneous connectivity with the additional bilateral projection between A and B ($f_0 = 20, f_{12} = f_{21} = 30$).

tance. The histograms in figure 4 show the timing distribution between sites A, B and sites A, C. The number of events has been restricted to $N = 675$ for both present and all following cases. The timing for A, B shows a clustering with broad wings around 50 time units ($dt = 0.025$ on a arbitrary scale), the timing for A, C shows a much broader distribution, even though there is a also a clustering around 50 time units observed. Note that the time period of a linear wave model, that is distance between A, B divided by velocity, falls into a similar regime implying that wave propagation mechanisms may contribute to the clustering in the distribution. Note also that the intrinsic time scale of the FHN model is in the same regime, that is $T = 80$ time units $= 2$.

4.2 Homogeneous connectivity and projection from A to B

In addition to the previous situation, a direct pathway is introduced from A to B providing an additional strengthening of the communication between these areas, but only uni-directional. Surprisingly, the variability in the timing between these areas does actually not change qualitatively compared to the purely homogeneous connectivity. No significant changes of the timing distribution can be observed between A, C either.

4.3 Homogeneous connectivity and bilateral pathway between A and B

The introduction of a bilateral fiber track, i.e. feed forward and feed backward communication, enhances the robustness of the timing of spike firings significantly. Higher harmonics of the dominant timing difference around 50 time units are also clearly present. The timing distribution for the sites A, C becomes flat. This appears to be a consequence of the reduced variability in the timing of A, B which also may be interpreted as the signature of the proximity of the system to the point at which spatial patterns emerge oscillating over time with the sites of A and B in anti-phase. In the purely deterministic system, that is without noise, the origin is still stable. Note that global inhibition is present in the current formulation of the model, hence the spatially uniform pattern of organization is suppressed and higher order patterns, such as the present, may be observed.

4.4 Heterogeneous pathways only

Finally we consider the isolated pathway between A, B only, i.e. the homogeneous local connectivity is suppressed and all active units except A, B act independently. It is notable that a broad cluster-

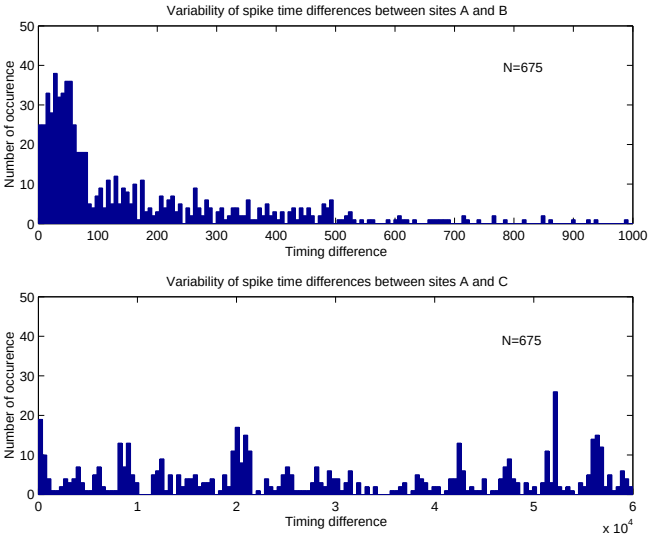

FIG. 7. Bilateral projections between A, C only ($f_0 = 0, f_{12} = f_{21} = 30$). All intermediate active units are independent.

ing is observed around the same time point as with the homogeneous connections in the previous case, but with a higher variability. We hypothesize that the additional mechanism of travelling wave propagation through the active medium contributes to a sharpening of the timing between distant sites which are directly connected with heterogeneous pathways. This result is surprising, in particular because both individual cases, heterogeneous projections only and homogeneous connectivity only, provide a broader distribution of timings independently. The variability of the timings between the sites A, C remains uniform as expected.

5 Summary

We described macroscopic coherent pattern formation in a spatially continuous system by means of an integral equation to capture effects caused by a heterogeneous connection topology. The connectivity serves as an intrinsic topological control parameter which systematically controls spatiotemporal bifurcations. We discussed how the introduction of an additional pathway connecting two distant sites may cause a phase transition and hence macroscopic pattern formation. Close to this threshold, we introduced noise into the system and studied the variability of the timings of events at different locations. It turns out that there is a parameter space for which the introduction of a unilateral pathway, from one site to the other, does not significantly alter the timing precision of events at the connected sites. However, the bilateral connection causes a significant reduction of the timing variability.

References

[1] H. Haken. *Synergetics. An Introduction.* 3rd ed. (Springer, Berlin, 1983).

[2] Haken H., Kelso J.A.S., Bunz H. A Theoretical Model of Phase transitions in Human Hand Movements. Biol. Cybern. **51**, 347 - 356 (1985)

[3] Haken H. *Principles of brain functioning.* (Springer, Berlin Heidelberg New York, 1996).

[4] M.C. Cross and P.C. Hohenberg. Rev. Mod. Phys. **65**, 851 (1993).

[5] M. Hendrey, E. Ott, T.M. Antonsen Jr. Phys.Rev.Lett. **82**, 859 (1999).

[6] G.B. Ermentrout and N. Kopell. SIAM J. Appl. Math. **54**, 478 (1994).

[7] V.K. Jirsa, J.A.S. Kelso. Phys.Rev E. **62**, 8462 (2000).

[8] V.K. Jirsa. Prog. Theor. Phys. Suppl. **139**, 128 (2000).

[9] S. Amari. Biol.Cybern. **27**, 77 (1977).

[10] P.L. Nunez. *Neocortical Dynamics and Human EEG Rhythms*, (Oxford University Press, 1995).

[11] V.K. Jirsa and H. Haken. Phys.Rev.Let. **77**, 960 (1996).

[12] J.J. Wright and D.T.J. Liley. Behav. Brain.Sci. **19**,285 (1996).

[13] P.A. Robinson, C.J. Rennie, J.J. Wright. Phys.Rev.E. **56**,826 (1997).

[14] R. FitzHugh. Biophys. J. **1**, 445 (1961)

[15] J. Nagumo, S. Arimoto, S. Yoshizawa. Proc. IRE. **50**, 2061 (1962).

[16] J.D. Murray. *Shape Mathematical Biology.* (Springer, Berlin Heidelberg New York, 1993).

[17] H.R. Wilson. *Shape Spikes, Decisions and Actions.* (Oxford University Press, 1999).